PFOS disrupts key developmental pathways during hiPSC-derived cardiomyocyte differentiation in vitro

Nichlas Davidsen, Louise Ramhøj, Indusha Kugathas, Bertrand Evrard, Thomas A Darde, Frédéric Chalmel, Terje Svingen, Anna Kjerstine Rosenmai

Toxicology in Vitro 85 (2022) 105475

Contents lists available at ScienceDirect

Toxicology in Vitro

journal homepage: www.elsevier.com/locate/toxinvit

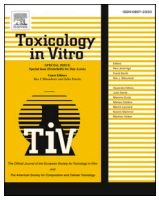

PFOS disrupts key developmental pathways during hiPSC-derived cardiomyocyte differentiation in vitro

Nichlas Davidsen [a,*], Louise Ramhøj [a], Indusha Kugathas [b], Bertrand Evrard [b], Thomas A. Darde [c], Frédéric Chalmel [b], Terje Svingen [a], Anna Kjerstine Rosenmai [a]

[a] National Food Institute, Technical University of Denmark, Kgs. Lyngby DK-2800, Denmark
[b] Univ Rennes, Inserm, EHESP, Irset (Institut de Recherche en Santé, Environnement et Travail), UMR_S 1085, F-35000 Rennes, France
[c] SciLicium, Rennes, France

ARTICLE INFO

Editor: Maxime Culot

Keywords:
Perfluorooctanesulfonic acid
In vitro
Spheroids
Development

ABSTRACT

Exposure to perfluorooctanesulfonic acid (PFOS) has been associated with congenital heart disease (CHD) and decreased birth weight. PFOS exposure can disrupt signaling pathways relevant for cardiac development in stem cell-derived cardiomyocyte assays, such as the PluriBeat assay, where spheroids of human induced pluripotent stem cells (hiPSCs) differentiate into contracting cardiomyocytes. Notably, cell line origin can also affect how the assay responds to chemical exposure. Herein, we examined the effect of PFOS on cardiomyocyte differentiation by transcriptomics profiling of two different hiPSC lines to see if they exhibit a common pattern of disruption. Two stages of differentiation were investigated: the cardiac progenitor stage and the cardiomyocyte stage. Many differentially expressed genes (DEGs) were observed between cell lines independent of exposure. However, 135 DEGs were identified as common between the two cell lines. Of these, 10 DEGs were associated with GO-terms related to the heart. PFOS exposure disrupted multiple signaling pathways relevant to cardiac development, including WNT, TGF, HH, and EGF. Of these pathways, genes related to the non-canonical WNT—Ca^{2+} signaling was particularly affected. PFOS thus has the capacity to disrupt pathways important for cardiac development and function.

1. Introduction

Perfluorooctanesulfonic acid (PFOS) belongs to a group of chemicals collectively known as *per-* and polyfluoroalkyl substances (PFASs). PFOS is readily detected in humans across the world (Kannan et al., 2004), attesting to widespread exposure in the general population. Since PFOS can pass the placental barrier (Gützkow et al., 2012), the unborn child is also at risk of exposure with potential negative consequences for normal development and lifelong health. For example, high levels of PFASs in maternal and cord blood serum is associated with decreased birthweight (Apelberg et al., 2007; Maisonet et al., 2012; Wikström et al., 2020), as well as congenital heart disease (CHD) at birth (Ou et al., 2021). These, and other, adverse developmental effects have also been demonstrated in animal studies (Thibodeaux et al., 2003; Xia et al., 2011; Zeng et al., 2015), which lends support to there being a direct link between PFAS exposure and adverse health outcomes in humans. The molecular basis for these PFAS-induced effects, however, is not well understood (Schrenk et al., 2020), although some studies suggest disruption to key developmental signaling pathways.

In human embryonic stem cell (hESC)-derived cardiomyocytes exposed to PFOS, transcriptomics analysis has revealed that PFOS promotes the formation of epicardial cells by disrupting WNT, IGF, FGF and BMP signaling (Yang et al., 2020). In differentiating cardiomyocytes from human induced pluripotent stem cells (hiPSCs), PFOS inhibits the formation of beating spheroids and disrupts the expression of the cardiac markers *Isl1* and *Myh7* (Davidsen et al., 2021). In mouse embryonic stem cells (mESCs), PFOS has been shown to disrupt cardiac differentiation by interfering with Rictor/mTORC2 signaling and induce abnormal sarcomere structures (Tang et al., 2017). In yet another mESC-derived cardiomyocyte study, PFOS reportedly increases expression of important cardiac markers such as *Nkx2.5* and *Myl4* (Cheng et al., 2013) and affects PPARα and MAPK-signaling (Zhang et al., 2016). Taken together, these studies suggest that PFOS and other PFASs can disrupt cardiomyocyte differentiation and thus contribute to the formation of CHDs.

To further explore how PFOS can disrupt cardiac development we

* Corresponding author.
E-mail address: nidav@food.dtu.dk (N. Davidsen).

https://doi.org/10.1016/j.tiv.2022.105475
Received 25 April 2022; Received in revised form 17 August 2022; Accepted 12 September 2022
Available online 16 September 2022

have performed extensive transcriptional profiling of the 3D culture hiPSC-derived cardiomyocyte assay PluriBeat, which uses a differentiation protocol to derive spheroids of contracting cardiomyocytes (Lauschke et al., 2020). We have previously shown that PFOS inhibits beat scores in this functional assay (Davidsen et al., 2021). Notably, however, cell donor origin can significantly affect stem cell assay outcomes (Rouhani et al., 2014), thus we explored PFOS-induced effects using two donors to potentially identify a shared mechanism of disruption, in order to identify common pathways and markers of effect on cardiomyocyte differentiation.

2. Materials and methods

2.1. Test substance

A stock solution of 200 μM of perfluorooctanesulfonic acid (PFOS) (98% purity, CAS# 2795-39-3, Sigma-Aldrich, USA) was prepared in dimethyl sulfoxide (DMSO) (Sigma-Aldrich, USA). Stocks were inspected visually to ensure solubility of the compound, before being stored at −20 °C.

2.2. Cell culture

Two hiPSC lines were used: BiONi010-C (Bioneer A/S, Denmark), which stems from the skin of a teenage male (Rasmussen et al., 2014) and IMR90–1 (WiCell, USA), which stems from lung tissue from a female fetus (Yu et al., 2007). Cells were cultured using mTeSR1 medium (Stemcell Technologies, USA) in 6 cm dishes coated with Matrigel (BD Biosciences, USA) at 37 °C and 5% CO_2. Cells were passaged once a week by washing with D-PBS (Sigma-Aldrich, USA) and treatment with 0.02% EDTA for 3 min using a split ratio of 1:10–1:40.

2.3. PluriBeat assay

The assay has previously been quality-assured using known teratogens such as thalidomide and epoxiconazole (Lauschke et al., 2020). Cardiomyocyte differentiation was conducted as previously described (Lauschke et al., 2020) (Fig. 1). Briefly, culture medium was removed from cells and the cell subsequently treated with 1 mL Gibco™ TrypleE™ Select (Gibco, USA). After 1 min of incubation, TrypLE was removed and a single cell suspension was made by adding mTeSR-ROCK medium (Davidsen et al., 2021). The composition of all the medium used in this protocol are in the supplemental material of Davidsen et al., 2021. Cells were seeded in 96-well Polystyrene Conical Bottom MicroWell™ Plates (Thermo Fisher Scientific, USA) maintaining a concentration of 5000 cells/well. The plates were centrifuged for 5 min at 500*g*, and set to incubate overnight at 37 °C with 5% CO_2 to promote embryoid body (EB) formation. The following day (D0), 80 μL of the mTeSR-Rock medium was replaced with 80 μL D0-medium. On day 1 (D1), 80 μL D0 medium was replaced with 80 μL TS-medium. Day 2, TS-medium was replaced with Wnt-medium. Day 3, Wnt-medium with TS-medium. And on day 6, 60 μL TS-medium was refreshed. PFOS were mixed with the medium from D1 through D6 with either DMSO (vehicle), 6.25 μM, 12.5 μM, or 25 μM PFOS, maintaining a solvent concentration of 0.1% in all treatments. PFOS concentrations were selected based on their ability to disturb cardiac differentiation without affecting other measures such as EB size (Davidsen et al., 2021). Each cell line was tested in five biological replicates (unique cell passages, $n = 5$) with 48 technical replicates per treatment group. Cells were harvested for RNA extraction at D3 and D7.

At assay termination (D7) EB beating was scored into three categories using a light microscope, and subsequently harvested for RNA extraction. Each well was evaluated for approximately 15 s and categorized according to their contractility. “Beat”: Contraction of the entire circumference of the EB. “Partial Beat”: EB contracts, but without moving the entire circumference. “No Beat”: No visible contraction. “No EB”: Missing or disintegrated EB. The experiment was only considered valid if 90% or more of the controls were categorized as beating (“Beat”).

EBs harvested for RNA extraction were pooled according to treatment groups at D3 (early stage) and D7 (late stage) for the five independent experiment ($n = 5$). Samples were centrifuged at 200*g* for 2 min at room temp. Medium was aspired carefully and samples frozen down to −80 °C.

Cell viability was not examined as this was assessed previously (Davidsen et al., 2021). All test concentrations were non-cytotoxic.

2.4. Beat score analysis

Statistical analysis of the beat score was conducted as described previously (Lauschke et al., 2020). The different categories were designated a score, “Beat” – 3, “Partial Beat” – 2, “No Beat” – 1, “No EB” – 0, to be used in the statistical analysis. Statistical significance was calculated using ordinal logistic regression in R with RStudio (RStudio inc, MA, USA). In this analysis, each EB is considered an individual unit, giving $n = 240$. Graphs were made using GraphPad Prism 8 (Graphpad Software, USA), showing the pooled distribution of the different beat categories in each treatment group.

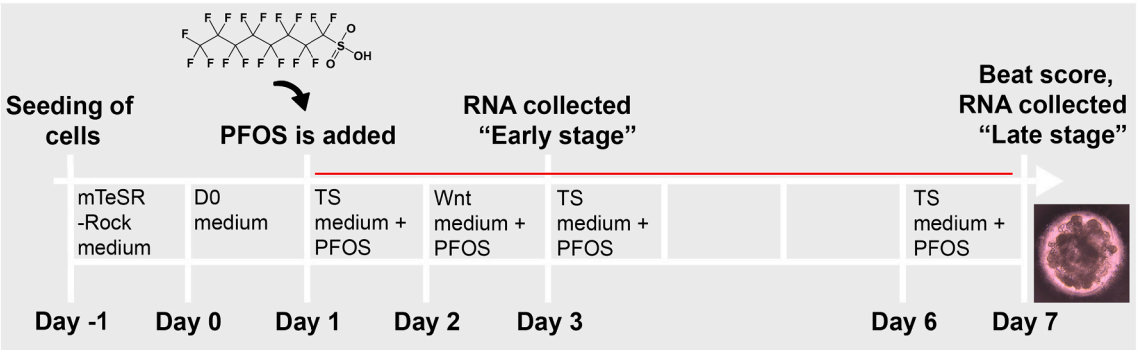

Fig. 1. PluriBeat protocol and study design. The pluriBeat assay was performed over a period of 8 days (indicated with vertical white lines). For each day, different differentiation medium was added to the culture. On “Day −1” cells were seeded into wells in mTeSR-Rock medium. The following day, “Day 0”, medium was exchanged with D0 medium. At “Day 1”, D0 medium was exchanged with TS medium containing PFOS; PFOS was added to the medium all the consecutive days. On “Day 2”, TS medium was exchanged with Wnt medium. On “Day 3” EBs of the “Early stage” of differentiation was collected, and Wnt medium was exchanged with TS medium. The cells were then left undisturbed over the weekend before TS medium was renewed on “Day 6”. On “Day 7”, the beat score was measured and the “Late stage” EBs were collected.

2.5. RNA isolation

Samples were thawed on ice and total RNA isolated using a Qiagen RNeasy micro kit (Qiagen, Hilden, Germany) with on-column DNase I treatment. Quantity and purity of RNA was measured with a nano-drop spectrometer (ND-1000, Fisher Scientific). The RNA samples were diluted to a concentration of 25 ng/μL in a 96-well PCR plate and stored at −80 °C for library preparation and sequencing.

2.6. Bulk RNA barcoding (BRB) library preparation and sequencing

The transcriptomic analysis was conducted using 3' Bulk RNA Barcoding and Sequencing (BRB-seq) (Alpern et al., 2019). The library was developed as previously described in Giacosa et al., 2021. In brief, 4 μL total RNA with a concentration of 2.5 ng/μL was used for initial reverse transcription and template switching. Double-stranded (ds) cDNAs were made with PCR using the purified cDNA. Sequencing libraries were built by tagmentation using 50 ng ds cDNA with an Illumina Nextera XT Kit (Illumina, #FC-131-1024) according to the manufacturer's recommendations. The resulting library was sequenced with an Illumina NovaSeq 6000 sequencing system. Base calling and image analysis was conducted using RTA 2.7.7 and bcl2fastq 2.17.1.14. Adapted dimer reads were removed using DimerRemover (https://sourceforge.net/projects/dimerremover/).

2.7. BRB-seq preprocessing and analysis

Preprocessing of raw data was conducted according to the quality control pipeline described in Giacosa et al., 2021. Initially, 16 bases are read and a quality score > 10 is ensured. The unique sample-specific barcode is assigned to the first 6 bp, and the unique molecular identifier (UMI) is assigned to the following 10 bp. Second reads were aligned using the human reference transcriptome from the UCSC website (hg38) with BWA version 0.7.4.4 and parameter "-l 24". Read mapping to multiple positions in the genome was removed from the analysis. A gene count matrix was made from UMIs associated with each gene (lines) in each sample (columns) following quality control and preprocessing of the data. The UMI matrix was normalized with regularized log (rlog) transformation package from DeSeq2 (Love et al., 2014). Raw and preprocessed data were deposited at the GEO repository under the accession number GSE202077 (Edgar et al., 2002).

2.8. Differential gene expression and functional analysis

The AMEN suite was used to identify differentially expressed genes (DEGs) (Chalmel and Primig, 2008). For each stage (early or late) of each cell line (BiONi010-C or IMR90–1) a statistical comparison between controls and the PFOS treated groups were made to identify DEGs. In short, genes that were more highly expressed than the background cutoff (overall median of rlog-transformed UMI dataset, 0.0) and that exceeded 1.5-fold change compared to the control were used for further analysis (Fig. 3, panels A-F). Significantly differentially expressed genes (DEGs) were finally identified by using the empirical Bayes moderated t-statistics implemented into the LIMMA package with an adjusted F-values estimated using Benjamini & Hochberg (BH) False Discovery rate approach ($p \leq 0.05$) (Ritchie et al., 2015; Smyth, 2004). Partitioning of the DEGs were performed by using the k-means method. Expression profiles of DEGs were displayed as false-colour heatmaps using the pheatmap package. Functional analyses were performed with AMEN (Chalmel and Primig, 2008) with FDR-adjusted p value of ≤ 0.05. The resulting toxicogenomics signatures were submitted to the TOXsIgN repository with the accession number TSP1268 (https://toxsign.genouest.org) (Darde et al., 2018).

3. Results

3.1. PFOS reduced beat score in both cell lines

We differentiated two hiPSC lines into contracting cardiomyocytes while concomitantly exposing them to PFOS for 6 days. In both cell lines, PFOS reduced the number of beating EBs significantly at all concentrations (Fig. 2). In the BiONi010-C cells, the response in beat decreased dose-dependently, reaching a 90% reduction compared to controls at 25 μM. In the IMR90–1 cells, the beat was reduced with approximately 25% in all treatments. These results from the BiONi010-C cells are consistent with our previous work (Davidsen et al., 2021).

3.2. Transcriptional effects by differentiation stage and cell line

We used BRB-seq to obtain hiPSC-cardiomyocyte transcriptomes in control and PFOS-exposed cells at both 'early' and 'late' stages of differentiation. Both the developmental stage and cell line were major factors affecting the transcriptome. When comparing the two stages for each cell line, 2,644 and 2,620 DEGs were found between the early and late stages in BiONi010-C and IMR90–1, respectively (Fig. 3A). When pooling the DEGs from both cell lines, a total of 3,835 unique DEGs were identified, suggesting that there are many overlapping genes, but also many that are unique for each cell line. We then directly compared the cell lines in non-treated conditions and found 3,540 DEGs between non-treated BiONi010-C and IMR90–1 (2,153 DEGs at early stage and 2,615 DEGs at the late stage) (Fig. 3B). In total, we defined a dynamic transcriptional landscape composed of 5,197 genes differentially expressed over time and/or between the two hiPS cell lines (Fig. 3, panels A-B; S1_Differentially_Expressed_Genes). Those DEGs were subsequently clustered into eight expression patterns (P1-P8) (Fig. 4A). Functional analysis revealed 1,610 enriched GO terms to be significantly associated with those eight patterns (S2_Controls_Functional_Analysis, Fig. 4B). Examining the heatmap more closely, there are several patterns where it appears that the main driver of differences in expression levels is the cell line (P1, P3, P4, P5, P7, and P8). For example, in the BiONi010-C cell line the patterns P1 and P5 are exclusively induced at the early and late

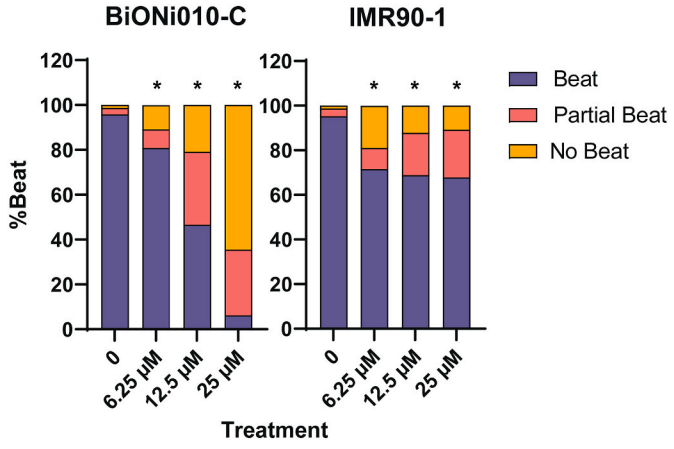

Fig. 2. PFOS disrupts differentiation of cardiomyocytes into beating cardiomyocytes. Two individual cell lines, BiONi010-C and IMR90–1, were differentiated into beating cardiomyocytes over an 8 day period. Simultaneously, the cells were treated with PFOS at concentrations of 0, 6.25, 12.5, and 25 μM from differentiation day D1-D7 of the protocol. At assay termination, cells were categorized into *Beat* (purple), *Partial Beat* (red), and *No Beat* (yellow). Each category was normalized the total number of EBs. Graphs represent 5 independent experiments with 48 technical replicates per treatment condition ($n = 240$). Statistically significant results are presented with (*) as determined with ordinal logistic regression with $p < 0.05$. (For interpretation of the references to colour in this figure legend, the reader is referred to the web version of this article.)

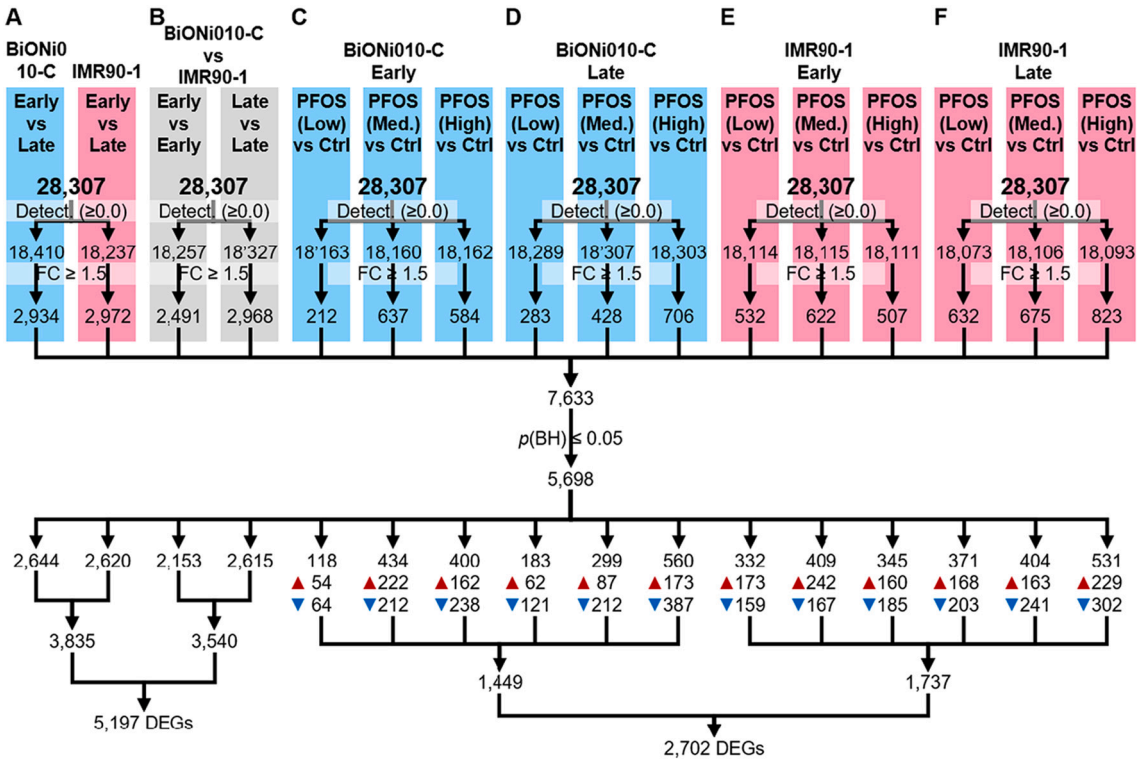

Fig. 3. Differentially expressed genes (DEGs) in each treatment group of each differentiation stage in two cell lines (BiONi010-C and IMR90-1). RNA was isolated from pooled EBs of each treatment group ($n = 5$), in both early and late stage of differentiation, for BiONi010-C (blue columns) and IMR90–1 (pink columns). The treatment concentrations correspond to; Ctrl: Vehicle (DMSO), PFOS (Low): 6.25 μM, PFOS (Med.): 12.5 μM, and PFOS (High): 25 μM. Each number outlines the DEGs identified when: (A) Comparing the early stage with the late stage in BiONi010-C or IMR90–1. (B) Comparing the early:early and late:late between BiONi010-C and IMR90–1. (C) Comparing the controls with PFOS treated BiONi010-C cells at the early stage. (D) Comparing controls with PFOS treated BiONi010-C cells at the late stage. (E) Comparing the controls with PFOS treated IMR90–1 cells at the early stage. (F) Comparing the controls with PFOS treated IMR90–1 cells at the late stage. The threshold for identifying DEGs was set to ≥1.5 fold-change (FC) and significance was determined using an adjusted *p*-value of ≤0.05. The lower part of the figure shows a breakdown into upregulated (red arrow) and downregulated (blue arrow) DEGs. Each column projects downwards and represent a specific comparison under the same experimental condition. (For interpretation of the references to colour in this figure legend, the reader is referred to the web version of this article.)

stage, respectively. Similarly, P7 and P8 are composed of genes exclusively expressed in IMR90–1 at the early and late stage, respectively. The associated GO-terms are related to different biological functions and processes such as embryo development in P1 (GO:0009790, *p*-value = 2E-3, 48 DEGs), gene expression in P3 (GO:0010467, 0.02, 399) and cytoplasm in P8 (GO:0005737, 3E-4, 313). Comparatively, P2 and P6 have a markedly different profile. Here, it appears that the expression level is comparable between the two donors and differences are mainly driven by differentiation stage, from high expression (early) to low expression (late) for P2, and vice versa for P6. P2 show enriched GO terms such as in utero embryonic development (GO:0001701, 0.03, 26) and anatomical structure homeostasis (GO:0060249, 0.04, 32). While in P6, there are several GO-terms related to the heart (contraction, development, cardiomyocyte differentiation), with the terms heart contraction (GO:0060047, 6E-19, 58), heart development (GO:0007507, 9E-21, 88), and cardiocyte differentiation (GO:0035051, 1E-11, 33). These two patterns indicate that certain processes are unified in the two cell lines. This may be tied to the differentiation program. This is especially evident for P6, which have multiple enriched terms associated with cardiac development.

3.3. PFOS induced massive transcriptional changes during differentiation

PFOS exposure induced 2,702 DEGs (Fig. 3C-F). The number of DEGs were similar between the early stage and late stage, but the majority of DEGs were unique to each stage. All the identified DEGs can be found in the supplemental material "S1_Differentially_Expressed_Genes".

There were differences in both expression (e.g. upregulation/downregulation) and expressional profile with increasing levels of exposure (e.g. dose-response/non-monotonic). Hence, there were few consistent DEGs between the two cell lines. Despite these differences, the functional analysis revealed that PFOS affected similar biological processes in both cell lines (Fig. 5B; S3_PFOS_Exposed_Functional_Analysis). Thus, there were significant enrichments of biological processed related to regulation of primary metabolic process (GO:0080090), cell differentiation (GO:0030154), cellular developmental process (GO:0070887), cellular response to chemical stimulus (GO:0070887) and regulation of signaling (GO:0023051) across almost all different stages and cell lines. In addition, cardiac development and function seemed to be similarly affected in the late stage of both cell lines, with enrichment of cardiac cell development (GO:0055006), cardiac muscle cell contraction (GO:0060048), heart development (GO:0007507), heart process (GO:0003015), myofibril (GO:0030016), and sarcomere (GO:0030017). The specific number of genes and *p*-values can be found in the supplementary table "S3_PFOS_Exposed_Functional_Analysis". This suggests that, although there are large differences in the genes affected by PFOS in both cell lines, they are still involved in similar processes. This indicates that the biological response to PFOS is almost similar across cell lines and that it is relevant to identify consistent pathways of these effects.

3.4. Identification of a shared pattern of PFOS exposure

We next tried to identify all DEGs that were affected similarly in both cell lines in at least one stage and one dose in response to PFOS exposure. This strategy identified 135 DEGs (Fig. 6A). Functional analysis showed

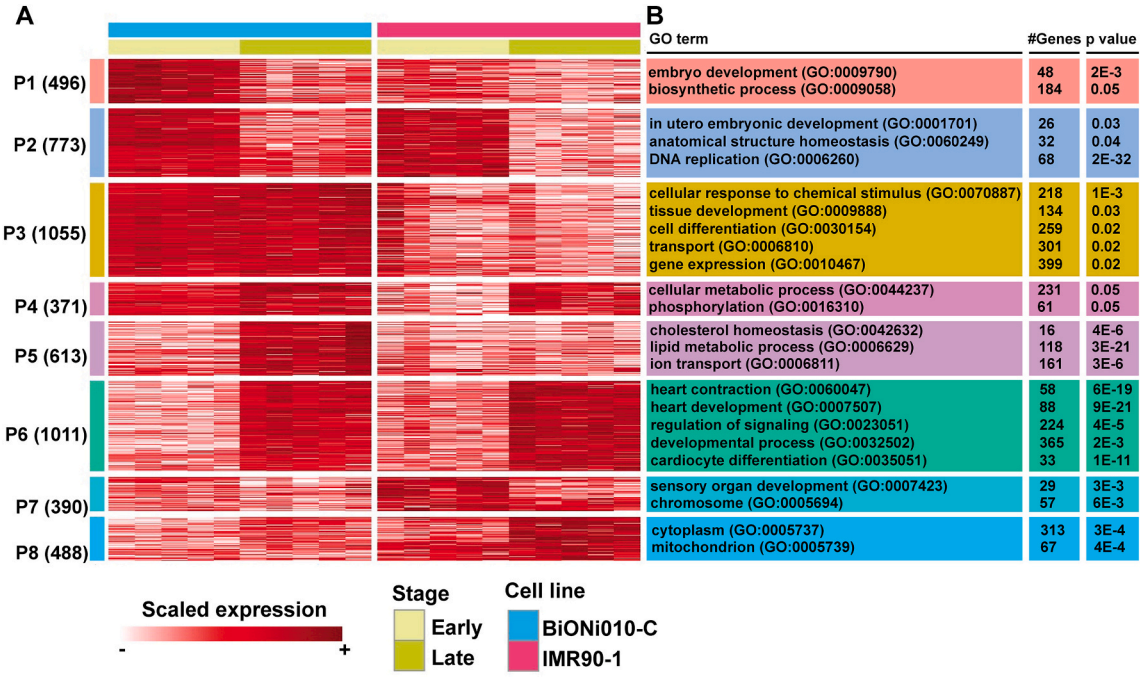

Fig. 4. Differentially expressed genes (DEGs) between controls BiONi010-C and IMR90–1 cell lines over time and associated GO-terms. Samples for transcriptomics were collected at an early and late stage of the PluriBeat differentiation protocol in two cell lines. (A) Heatmap of DEGs derived from comparison between cell line (BiONi010-C (blue) and IMR90–1 (pink)) and between differentiation stage (early (light green) and late (dark green)) clustered into eight distinct patterns, P1-P8. The scaled expression of each single gene is shown as a gradient from white (−) to red (+). (B) A selection of enriched GO terms from each pattern shown together with number of affected genes and adjusted p-value. (For interpretation of the references to colour in this figure legend, the reader is referred to the web version of this article.)

that PFOS across cell lines affects the expression of genes related to regulation of developmental process (GO:0050793, p value <0.02, 35 genes) and cell differentiation (GO:0030154, 9E-3, 50) (Fig. 6B). Importantly, PFOS exposures also causes transcriptional changes in genes involved in cardiac development and function. Ten of the genes are listed in at least one cardiac or heart related GO term when cross referenced with the Ensemble database (Cunningham et al., 2022) (Fig. 6C).

4. Discussion

We sought to identify a shared transcriptomic profile of PFOS-induced disruption of cardiomyocyte differentiation. To do this, we exposed hiPSCs originating from two different donors to PFOS whilst differentiating into beating cardiomyocytes. Transcriptomics analysis was conducted at two stages of development, corresponding to cardiac progenitors (early stage) and developed cardiomyocytes (late stage) (Lauschke et al., 2020). With this approach it became apparent that the transcriptional landscape between cell lines originating from different donors can vary significantly. This fact warrants further scrutiny, especially if including expression profiling in effect outcome measurements. Notably, the BiONi010-C cells originate from a male teenager, whereas the IMR90–1 cells originate from a female fetus, highlighting that cell line origin can play a critical role in toxicological responses, also in vitro (Rouhani et al., 2014).

Functional analysis indicated that key pathways central to the assay was conserved at both stages in both cell lines, as several GO terms related to cardiac development and function was enriched of genes exhibiting slight transcriptional changes between both cell lines. This serves to both validate the experimental model, as we know that the EBs functionally differentiate into beating cardiomyocytes during the time frame of the experiment, and to show that the pattern containing the GO-terms relevant for the functional output of the PluriBeat assay is highly similar in both cell lines.

We chose to focus largely on shared effect patterns from PFOS exposure. Despite the high variation between the cell lines, we identified 135 common DEGs that shared the same expressional trend under the same experimental conditions. Functional analysis of these 135 DEGs uncovered few and rather unspecific GO terms due to the low number of DEGs. The BiONi010-C cells displayed a decreasing level of beat with increasing levels of PFOS exposure, whereas the imr90–1 cell line displayed significant effects at the same concentrations, but the maximum effect was less pronounced, and no concentration-dependent response was observed. This trend was less visible when evaluating the transcriptome, in which both cell lines have comparable number of identified DEGs in the PFOS exposed groups.

Many of the PFOS-induced DEGs shared between the two cell lines were related to cardiac development, including *Foxc1*, *Hmga2*, *Alcam*, and *Hhip and Hhatl* (Gessert et al., 2008; Gripp et al., 2013; Lee et al., 2017; Monzen et al., 2008; Wiegering et al., 2017). This indicates that PFOS may interfere with cardiac differentiation and affect lineage specification. Among these, *Foxc1*, a gene commonly associated with congenital heart disease (CHD) in humans (Gripp et al., 2013; Khalil et al., 2017; Zhu, 2016) was downregulated at the early stage. *Foxc1* plays an important role in the formation of the cardiac mesoderm and directly regulates the expression of the cardiac markers, such as *Myh7* (Lambers et al., 2016). Multiple genes related to regulation of cardiac hypertrophy and stress response in the heart were also affected, such as *Camk2a, Hmga2*, *Rgs4*, Fhl2, *Nup155*, *Usp19*, *Ppp1r12b*, *Hhatl*, *Mlip,* and *Bambi* (Chiang et al., 2018; Hojayev et al., 2012; Kramerova et al., 2012; Miao et al., 2020; Mittmann et al., 2002; Monzen et al., 2008; Preston et al., 2018; Shi et al., 2021; Villar et al., 2013). Cardiac hypertrophy is a compensatory process which is recognized by increased cardiomyocyte size, protein synthesis, and changes in sarcomere organization. Cardiac hypertrophy is associated with a number of cardiac pathologies leading to cardiac failure (Frey and Olson, 2003). Collectively, the affected DEGs points to changes in the functional output, decreased beat, and suggest that many of these core genes should be examined for their potential as

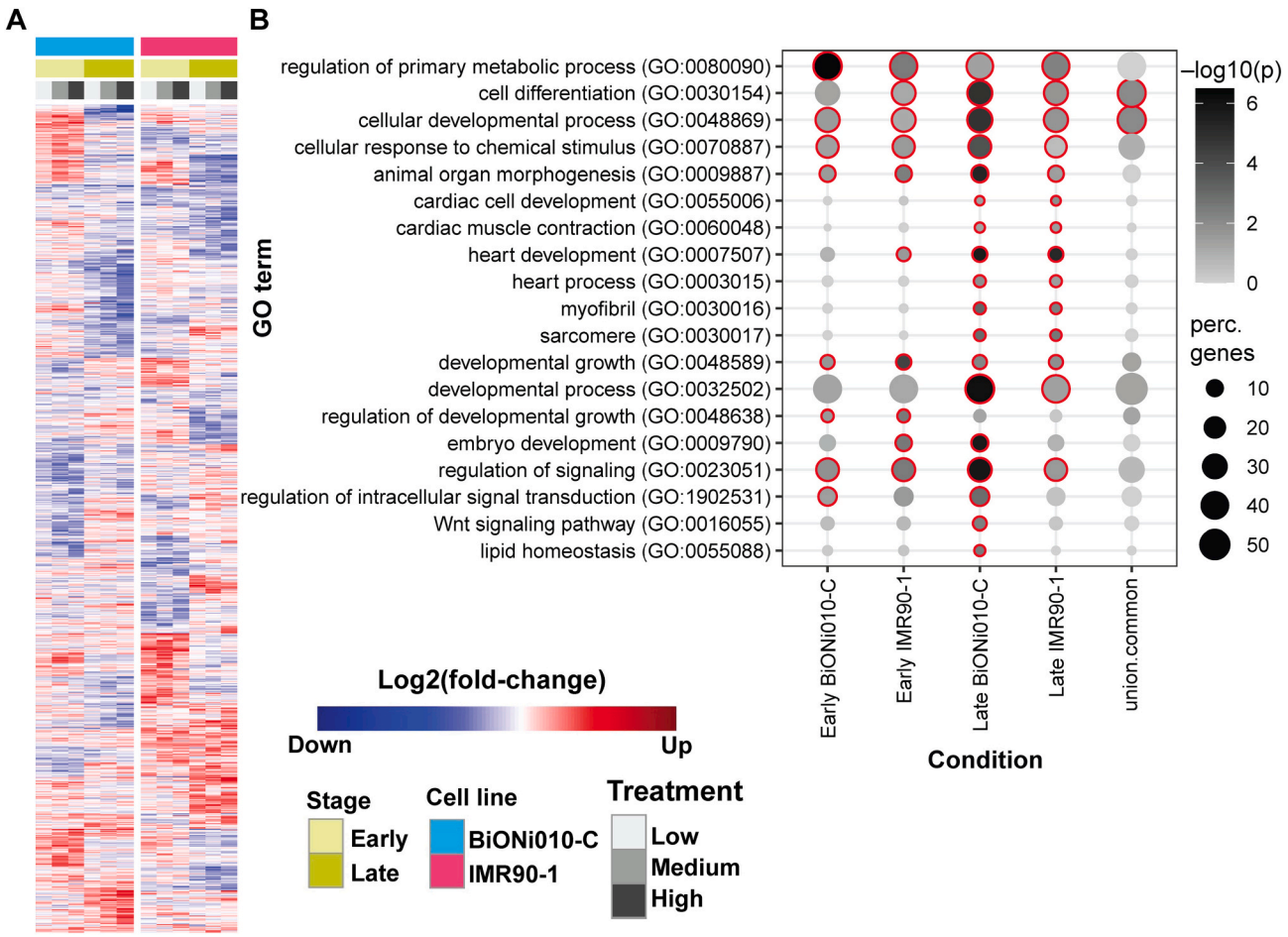

Fig. 5. DEGs identified in response to PFOS exposure in both BiONi010-C (blue) and IMR90–1 (pink) cell lines. Cells were exposed to PFOS for 6 days during the differentiation protocol to establishment of contracting cardiomyocytes. Samples for transcriptomics were collected after 2 (Early, light green) and 6 (Late, dark green) days of exposure to PFOS. The treatment concentrations used were; Ctrl: Vehicle (DMSO), PFOS (Low): 6.25 μM, PFOS (Med.): 12.5 μM, and PFOS (High): 25 μM. (A) Heatmap of the 2,702 DEGs identified when comparing the transcriptome of the PFOS treated groups with the controls. (B) Selection of GO terms and their level of enrichment in each group following PFOS exposure and overlapping genes between all the groups (union.common). Significance levels are given in scale of grey (−log10(p)). The percentage of associated DEGs in each GO term is indicated by the size of the circle (perc. genes). Red ring indicates significant enrichment (adj. *p* value of ≤0.05). (For interpretation of the references to colour in this figure legend, the reader is referred to the web version of this article.)

future candidates as PFAS, or general cardiotoxicity, biomarkers.

Many studies have investigated the effects of PFOS on cardiomyocyte cell systems and heart development (Cheng et al., 2013; Harada et al., 2006; Tang et al., 2017; Xia et al., 2011; Zhang et al., 2016). One transcriptomics study using human ESC-derived cardiomyocytes suggested that signaling pathways such as WNT, IGF, FGF, and BMP may be perturbed by PFOS (Yang et al., 2020). We also observe disruption to many of the same signaling pathways, though there are differences in the specific effects. For instance, Yang et al., 2020 reports that PFOS skews cardiomyocyte differentiation towards epicardial cells through upregulated WNT signaling, whereas we observed indications of downregulated WNT signaling. In fact, many of the DEGs identified herein were related to the WNT signaling pathway, including *Shisa2*, *Ppp2r2b*, *Alcam, Ppm1j*, *Caloco1, Cdc42se2 Capn3*, and *Camk2a*. The latter three genes were downregulated in both cell lines and are related to the non-canonical WNT—Ca^{2+} signaling pathway. *CaMK* plays a role in modulating gene expression, *Capn3* is an inducer of CaMKII signaling, and PKC-Cdc42 pathway is thought to play a role in cytoskeletal change during cardiac development (Kramerova et al., 2012; Ruiz-Villalba et al., 2016). Further, *Kcnmb1*, coding for a subunit of the calcium activated potassium (*MaxiK*) channel, was downregulated. This channel sensitivity is modulated by CamKII signaling (van Welie and du Lac, 2011). Finally, a repressor of WNT signaling, *Shisa2* was upregulated. Some of these genes are known to affect endpoints of relevance for heart function. For instance, knockout of *Capn3* causes abnormal sarcomere structures in mice (Kramerova et al., 2004), MaxiK channels may play a role in the sarcomere formation and electrical coupling in the embryonic heart (Niu et al., 2008), whereas *Shisa2* promotes myoblast fusion in skeletal muscle (Liu et al., 2018). Collectively, downregulation of *Camk2a* and the components of WNT signaling pathway with increases in upstream repressor of the pathway suggest a general downregulation of the WNT—Ca^{2+} pathway. This would lead to decreased intracellular Ca^{2+} levels, which could potentially affect differentiation, development, and cardiac hypertrophy (Ruiz-Villalba et al., 2016). Interestingly, PFOS can decreased Ca^{2+} flux in mESCs (Tang et al., 2017) and alter calcium homeostasis in guinea pigs (Harada et al., 2005), which are in line with our findings.

We also observed a downregulation of genes related to Hedgehog (HH) signaling, including *Hhip, Hhatl,* and *Iqce* (Lee et al., 2017; Pusapati et al., 2014; Shi et al., 2021), as well as upregulation of the HH repressor *Enpp1* (Jin et al., 2018). This suggests that PFOS can repress Hh signaling, a prominent regulatory pathway in cardiac development (Briscoe and Thérond, 2013; Wiegering et al., 2017). Knockout of Sonic hedgehog (*Shh*) in mice causes heart and septal defects (Smoak et al., 2005). *Hhip*, which inhibit stem cell progenitor function and differentiation (Lee et al., 2017), was downregulated at the early stage. *Hhip* is

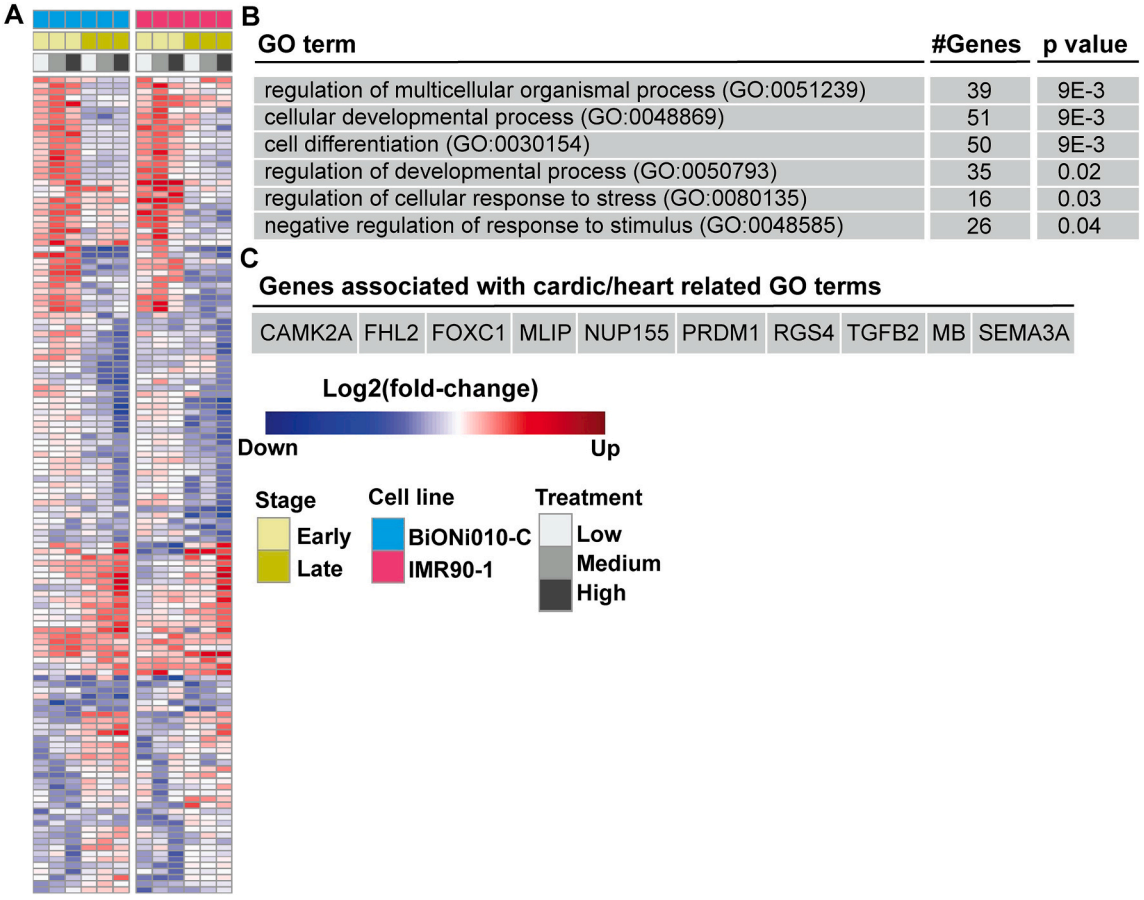

Fig. 6. Common DEGs between the two cell lines at same differentiation stage following PFOS exposure. Cells were exposed to PFOS for 6 days during the differentiation protocol to establishment of contracting cardiomyocytes. Samples for transcriptomics were collected after 2 (Early, light green) and 6 (Late, dark green) days of exposure to PFOS. The treatment concentrations were; Ctrl: Vehicle (DMSO), PFOS (Low): 6.25 μM, PFOS (Med.): 12.5 μM, and PFOS (High): 25 μM. (A) Heatmap of the 135 overlapping DEGs affected in both cell lines at same differentiation stage. (B) Enriched GO terms based on the 135 DEGs shown together with corresponding number of genes and adjusted p value. (C) Cardiac and heart related genes as identified by associated cardiac/heart related GO terms. (For interpretation of the references to colour in this figure legend, the reader is referred to the web version of this article.)

also associated with embryonic myogenesis (Mok et al., 2018). *Hhip* expression is induced by HH signaling, and repress Hh through a negative feedback loop (Chuang and McMahon, 1999). Similarly, oxidative stress and growth factors such as VEGF and FGF repress *Hhip* expression (Lee et al., 2017). Notably, *Hhatl* which can interact with Ca^{2+}-mediated signaling pathways, was downregulated at the late stage of cardiomyocyte differentiation, a pathway that also cross-talk with WNT signaling as discussed above. *Hhatl* is highly expressed in heart during embryonic development and blocking *Hhatl* expression causes cardiac defects (Shi et al., 2021).

Both cell lines exhibited increased expression of *Tgfb2* at the late stage, suggesting an activation of the TGF-β signaling pathway. Increased expression of TGF-β is commonly observed in patients and animal models with cardiac remodeling, hypertrophy and failure (Dobaczewski et al., 2011). Multiple signaling pathways are downstream of TGF-β, such as SMADs, MAPK, TAK1, Ras and Rho (Dobaczewski et al., 2011). At the transcript level there were no change in markers directly related to these pathways. However, multiple genes regulated by these pathways were affected, including MAPK signaling, with the genes *Sh3rf1*, *Gpm6a*, *Klhl31*, and *Scrib*. Similarly, PFOS disturbs MAPK signaling in mESCs differentiating to cardiomyocytes, resulting in disturbed cardiac differentiation (Zhang et al., 2016). In addition, a negative regulator of TGF- β signaling, *Bambi*, was upregulated at the late stage. Deletion of *Bambi* leads to upregulation of TGF-β through Smad and TAK1 signaling pathways, whereby it negatively modulates cardiac remodeling during pressure overload (Villar et al., 2013).

None of the genes that were affected in our previous study (Davidsen et al., 2021) were consistently affected in both cell lines herein. This could suggests that these are poor markers of PFOS-induced disruption of cardiomyocyte differentiation. This highlights the importance of using multiple cell lines to find transcriptomic profiles of effect in this type of study. We did, however, find a shared pattern of effect related to the non-canonical WNT—Ca^{2+} pathway. Similar effects had also been observed in mESCs and guinea pigs. This might suggest that this is a viable pathway for PFAS-related screening of cardiac related effects. However, further studies have to be conducted to solidify its relationship with cardiac malformations in vivo.

Reported human levels of PFOS are lower than the concentrations inducing effects here. For example, studies connecting PFAS exposure with CHDs report median PFOS levels of 5.8 ng/mL (0.012 μM) in the blood plasma of the mothers and 1.9 ng/mL (0.004 μM) in plasma samples from cord blood (Ou et al., 2021). Comparable levels of PFOS was not associated with incidence of spontaneous abortion in mothers with blood levels in the ranges of 2.36 ng/mL (0.005 μM, 25th percentile) and 6.57 ng/mL (0.013 μM, 75th percentile), with a median of 4.1 ng/mL (0.008 μM) (Nian et al., 2022). We previously determined the LOEC to be 3126 ng/mL PFOS (6.25 μM) in the cardiomyocyte assay (Davidsen et al., 2021). This is significantly higher than the levels reported in many of these epidemiological studies. However, cellular uptake of PFASs has been reported to be low in vitro. In cells exposed to 10 μM PFOS, only 0.04% was found to be retained in the cells (Rosenmai

et al., 2018). One explaining factor for this large discrepancy could be loss of PFOS to various laboratory equipment. PFOA, a compound structurally similar to PFOS, has been reported to adsorb to plastics such as polypropylene, leading to 32–45% loss of PFOA from an aqueous solution (Lath et al., 2019). Additionally, other PFASs may induce similar effects, as shown for PFOA (Davidsen et al., 2021), which in vivo may contribute to these effects together with other chemicals that humans are exposed to.

5. Conclusion

PFOS exposure can affect genes related to cardiac development and function, as well as cardiac hypertrophy and failure, which we observed in cardiomyocytes derived from two individual hiPS cell lines. This suggests that PFOS may be disruptive to both the developing and adult heart. To date, only one epidemiological study has found an association between CHDs and PFAS exposure (Ou et al., 2021). More work has to be conducted to understand the connection between PFASs and the development of CHD, and whether this could be a contributing factor to the observed decrease in birth weight. We found that PFOS can affect genes related to cardiac development, as well as cardiac hypertrophy, remodeling, and failure. Many of the affected genes were related to signaling pathways such as WNT, TGF, HH, EGF, and mTOR. The pathways affected are associated with the development of CHDs. Whether PFOS has one mechanism of action or multiple is hard to establish. In addition, with the current model system we cannot determine how these perturbations would affect structural development of the heart. However, PFOS disruption of differentiation was more unified in the late stage, indicating that cardiac differentiation may be the most sensitive to PFOS induced perturbation at this stage. The focus of future studies should be to find ways to connect these types of effects with those observed in more complex model systems and at the population level.

Funding

The project was funded by the Ministry of Food, Agriculture and Fisheries of Denmark, project FEMINIX. The funding sources had no involvement in the study design, data collection and analysis, or in the writing of this manuscript.

Declaration of Competing Interest

The authors declare that they have no known competing financial interests or personal relationships that could have appeared to influence the work reported in this paper.

Appendix A. Supplementary data

Supplementary data to this article can be found online at https://doi.org/10.1016/j.tiv.2022.105475.

References

Alpern, D., Gardeux, V., Russeil, J., Mangeat, B., Meireles-Filho, A.C.A., Breysse, R., Hacker, D., Deplancke, B., 2019. BRB-seq: ultra-affordable high-throughput transcriptomics enabled by bulk RNA barcoding and sequencing. Genome Biol. 201 (20), 1–15. https://doi.org/10.1186/S13059-019-1671-X.

Apelberg, B.J., Witter, F.R., Herbstman, J.B., Calafat, A.M., Halden, R.U., Needham, L.L., Goldman, L.R., 2007. Cord serum concentrations of perfluorooctane sulfonate (PFOS) and perfluorooctanoate (PFOA) in relation to weight and size at birth. Environ. Health Perspect. 115, 1670–1676. https://doi.org/10.1289/ehp.10334.

Briscoe, J., Thérond, P.P., 2013. The mechanisms of hedgehog signalling and its roles in development and disease. Nat. Rev. Mol. Cell Biol. 147 (14), 416–429. https://doi.org/10.1038/NRM3598.

Chalmel, F., Primig, M., 2008. The annotation, mapping, expression and network (AMEN) suite of tools for molecular systems biology. BMC Bioinformatics 9. https://doi.org/10.1186/1471-2105-9-86.

Cheng, W., Yu, Z., Feng, L., Wang, Y., 2013. Perfluorooctane sulfonate (PFOS) induced embryotoxicity and disruption of cardiogenesis. Toxicol. in Vitro 27, 1503–1512. https://doi.org/10.1016/j.tiv.2013.03.014.

Chiang, D.Y., Alsina, K.M., Corradini, E., Fitzpatrick, M., Ni, L., Lahiri, S.K., Reynolds, J. O., Pan, X., Scott, L., Heck, A.J.R., Wehrens, X.H.T., 2018. Rearrangement of the protein phosphatase 1 interactome during heart failure progression. Circulation 138, 1569–1581. https://doi.org/10.1161/CIRCULATIONAHA.118.034361.

Chuang, P.T., McMahon, A.P., 1999. Vertebrate hedgehog signalling modulated by induction of a hedgehog-binding protein. Nat 397, 617–621. https://doi.org/10.1038/17611.

Cunningham, F., Allen, J.E., Allen, J., Alvarez-Jarreta, J., Amode, M.R., Armean, I.M., Austine-Orimoloye, O., Azov, A.G., Barnes, I., Bennett, R., Berry, A., Bhai, J., Bignell, A., Billis, K., Boddu, S., Brooks, L., Charkhchi, M., Cummins, C., Da Rin Fioretto, L., Davidson, C., Dodiya, K., Donaldson, S., El Houdaigui, B., El Naboulsi, T., Fatima, R., Giron, C.G., Genez, T., Martinez, J.G., Guijarro-Clarke, C., Gymer, A., Hardy, M., Hollis, Z., Hourlier, T., Hunt, T., Juettemann, T., Kaikala, V., Kay, M., Lavidas, I., Le, T., Lemos, D., Marugán, J.C., Mohanan, S., Mushtaq, A., Naven, M., Ogeh, D.N., Parker, A., Parton, A., Perry, M., Pilizota, I., Prosovetskaia, I., Sakthivel, M.P., Salam, A.I.A., Schmitt, B.M., Schuilenburg, H., Sheppard, D., Perez-Silva, J.G., Stark, W., Steed, E., Sutinen, K., Sukumaran, R., Sumathipala, D., Suner, M.M., Szpak, M., Thormann, A., Tricomi, F.F., Urbina-Gómez, D., Veidenberg, A., Walsh, T.A., Walts, B., Willhoft, N., Winterbottom, A., Wass, E., Chakiachvili, M., Flint, B., Frankish, A., Giorgetti, S., Haggerty, L., Hunt, S.E., Iisley, G.R., Loveland, J.E., Martin, F.J., Moore, B., Mudge, J.M., Muffato, M., Perry, E., Ruffier, M., Tate, J., Thybert, D., Trevanion, S.J., Dyer, S., Harrison, P.W., Howe, K.L., Yates, A.D., Zerbino, D.R., Flicek, P., 2022. Ensembl 2022. Nucleic Acids Res. 50, D988–D995. https://doi.org/10.1093/NAR/GKAB1049.

Darde, T.A., Gaudriault, P., Beranger, R., Lancien, C., Caillarec-Joly, A., Sallou, O., Bonvallot, N., Chevrier, C., Mazaud-Guittot, S., Jégou, B., Collin, O., Becker, E., Rolland, A.D., Chalmel, F., 2018. TOXsIgN: a cross-species repository for toxicogenomic signatures. Bioinformatics 34, 2116–2122. https://doi.org/10.1093/BIOINFORMATICS/BTY040.

Davidsen, N., Rosenmai, A.K., Lauschke, K., Svingen, T., Vinggaard, A.M., 2021. Developmental effects of PFOS, PFOA and GenX in a 3D human induced pluripotent stem cell differentiation model. Chemosphere 279, 130624. https://doi.org/10.1016/J.CHEMOSPHERE.2021.130624.

Dobaczewski, M., Chen, W., Frangogiannis, N.G., 2011. Transforming growth factor (TGF)-β signaling in cardiac remodeling. J. Mol. Cell. Cardiol. 51, 600. https://doi.org/10.1016/J.YJMCC.2010.10.033.

Edgar, R., Domrachev, M., Lash, A.E., 2002. Gene expression omnibus: NCBI gene expression and hybridization array data repository. Nucleic Acids Res. 30, 207–210. https://doi.org/10.1093/NAR/30.1.207.

Frey, N., Olson, E.N., 2003. Cardiac Hypertrophy: The Good, The Bad, and The Ugly. doi: https://doi.org/10.1146/annurev.physiol.65.092101.142243 65, 45–79. doi: https://doi.org/10.1146/ANNUREV.PHYSIOL.65.092101.142243.

Gessert, S., Maurus, D., Brade, T., Walther, P., Pandur, P., Kühl, M., 2008. DM-GRASP/ALCAM/CD166 is required for cardiac morphogenesis and maintenance of cardiac identity in first heart field derived cells. Dev. Biol. 321, 150–161. https://doi.org/10.1016/J.YDBIO.2008.06.013.

Giacosa, S., Pillet, C., Séraudie, I., Guyon, L., Wallez, Y., Roelants, C., Battail, C., Evrard, B., Chalmel, F., Barette, C., Soleilhac, E., Fauvarque, M.O., Franquet, Q., Sarrazin, C., Peilleron, N., Fiard, G., Long, J.A., Descotes, J.L., Cochet, C., Filhol, O., 2021. Cooperative blockade of CK2 and ATM kinases drives apoptosis in VHL-deficient renal carcinoma cells through ROS overproduction. Cancers 13, 576 (13, 576). https://doi.org/10.3390/CANCERS13030576.

Gripp, K.W., Hopkins, E., Jenny, K., Thacker, D., Salvin, J., 2013. Cardiac anomalies in Axenfeld–Rieger syndrome due to a novel FOXC1 mutation. Am. J. Med. Genet. Part A 161, 114–119. https://doi.org/10.1002/AJMG.A.35697.

Gützkow, K.B., Haug, L.S., Thomsen, C., Sabaredzovic, A., Becher, G., Brunborg, G., 2012. Placental transfer of perfluorinated compounds is selective - a Norwegian mother and child sub-cohort study. Int. J. Hyg. Environ. Health 215, 216–219. https://doi.org/10.1016/j.ijheh.2011.08.011.

Harada, K., Xu, F., Ono, K., Iijima, T., Koizumi, A., 2005. Effects of PFOS and PFOA on L-type Ca2+ currents in guinea-pig ventricular myocytes. Biochem. Biophys. Res. Commun. 329, 487–494. https://doi.org/10.1016/J.BBRC.2005.01.163.

Harada, K.H., Ishii, T.M., Takatsuka, K., Koizumi, A., Ohmori, H., 2006. Effects of perfluorooctane sulfonate on action potentials and currents in cultured rat cerebellar Purkinje cells. Biochem. Biophys. Res. Commun. 351, 240–245. https://doi.org/10.1016/J.BBRC.2006.10.038.

Hojayev, B., Rothermel, B.A., Gillette, T.G., Hill, J.A., 2012. FHL2 binds Calcineurin and represses pathological cardiac growth. Mol. Cell. Biol. 32, 4025. https://doi.org/10.1128/MCB.05948-11.

Jin, Y., Cong, Q., Gvozdenovic-Jeremic, J., Hu, J., Zhang, Y., Terkeltaub, R., Yang, Y., 2018. Enpp1 inhibits ectopic joint calcification and maintains articular chondrocytes by repressing hedgehog signaling. Development 145. https://doi.org/10.1242/DEV.164830.

Kannan, K., Corsolini, S., Falandysz, J., Fillmann, G., Kumar, K.S., Loganathan, B.G., Mohd, M.A., Olivero, J., Van Wouwe, N., Yang, J.H., Aldous, K.M., 2004. Perfluorooctanesulfonate and related fluorochemicals in human blood from several countries. Environ. Sci. Technol. 38, 4489–4495. https://doi.org/10.1021/es0493446.

Khalil, A., Al-Haddad, C., Hariri, H., Shibbani, K., Bitar, F., Kurban, M., Nemer, G., Arabi, M., 2017. A novel mutation in FOXC1 in a Lebanese family with congenital heart disease and anterior segment dysgenesis: potential roles for NFATC1 and DPT in the phenotypic variations. Front. Cardiovasc. Med. 4, 20. https://doi.org/10.3389/FCVM.2017.00058/FULL.

Kramerova, I., Kudryashova, E., Tidball, J.G., Spencer, M.J., 2004. Null mutation of calpain 3 (p94) in mice causes abnormal sarcomere formation in vivo and in vitro. Hum. Mol. Genet. 13, 1373–1388. https://doi.org/10.1093/HMG/DDH153.

Kramerova, I., Kudryashova, E., Ermolova, N., Saenz, A., Jaka, O., López De Munain, A., Spencer, M.J., 2012. Impaired calcium calmodulin kinase signaling and muscle adaptation response in the absence of calpain 3. Hum. Mol. Genet. 21, 3193. https://doi.org/10.1093/HMG/DDS144.

Lambers, E., Arnone, B., Fatima, A., Qin, G., Andrew Wasserstrom, J., Kume, T., 2016. Foxc1 regulates early Cardiomyogenesis and functional properties of embryonic stem cell derived cardiomyocytes. Stem Cells 34, 1487–1500. https://doi.org/10.1002/STEM.2301.

Lath, S., Knight, E.R., Navarro, D.A., Kookana, R.S., McLaughlin, M.J., 2019. Sorption of PFOA onto different laboratory materials: filter membranes and centrifuge tubes. Chemosphere 222, 671–678. https://doi.org/10.1016/j.chemosphere.2019.01.096.

Lauschke, K., Rosenmai, A.K., Meiser, I., Neubauer, J.C., Schmidt, K., Rasmussen, M.A., Holst, B., Taxvig, C., Emnéus, J.K., Vinggaard, A.M., 2020. A novel human pluripotent stem cell-based assay to predict developmental toxicity. Arch. Toxicol. 1, 3. https://doi.org/10.1007/s00204-020-02856-6.

Lee, B.N.R., Son, Y.S., Lee, D., Choi, Y.J., Kwon, S.M., Chang, H.K., Kim, P.H., Cho, J.Y., 2017. Hedgehog-interacting protein (HIP) regulates apoptosis evasion and Angiogenic function of late endothelial progenitor cells. Sci. Reports 71 (7), 1–11. https://doi.org/10.1038/s41598-017-12571-5.

Liu, Z., Wang, C., Liu, X., Kuang, S., 2018. Shisa2 regulates the fusion of muscle progenitors. Stem Cell Res. 31, 31–41. https://doi.org/10.1016/J.SCR.2018.07.004.

Love, M.I., Huber, W., Anders, S., 2014. Moderated estimation of fold change and dispersion for RNA-seq data with DESeq2. Genome Biol. 15, 1–21. https://doi.org/10.1186/S13059-014-0550-8/FIGURES/9.

Maisonet, M., Terrell, M.L., McGeehin, M.A., Christensen, K.Y., Holmes, A., Calafat, A. M., Marcus, M., 2012. Maternal concentrations of polyfluoroalkyl compounds during pregnancy and fetal and postnatal growth in british girls. Environ. Health Perspect. 120, 1–26. https://doi.org/10.1289/ehp.1003096.

Miao, R., Lu, Y., He, X., Liu, X., Chen, Z., Wang, J., 2020. Ubiquitin-specific protease 19 blunts pathological cardiac hypertrophy via inhibition of the TAK1-dependent pathway. J. Cell. Mol. Med. 24, 10946. https://doi.org/10.1111/JCMM.15724.

Mittmann, C., Chung, C.H., Höppner, G., Michalek, C., Nose, M., Schüler, C., Schuh, A., Eschenhagen, T., Weil, J., Pieske, B., Hirt, S., Wieland, T., 2002. Expression of ten RGS proteins in human myocardium: functional characterization of an upregulation of RGS4 in heart failure. Cardiovasc. Res. 55, 778–786. https://doi.org/10.1016/S0008-6363(02)00459-5/2/55-4-778-FIG 5.GIF.

Mok, G.F., Lozano-Velasco, E., Maniou, E., Viaut, C., Moxon, S., Wheeler, G., Münsterberg, A., 2018. miR-133-mediated regulation of the hedgehog pathway orchestrates embryo myogenesis. Development 145. https://doi.org/10.1242/DEV.159657.

Monzen, K., Ito, Y., Naito, A.T., Kasai, H., Hiroi, Y., Hayashi, D., Shiojima, I., Yamazaki, T., Miyazono, K., Asashima, M., Nagai, R., Komuro, I., 2008. A crucial role of a high mobility group protein HMGA2 in cardiogenesis. Nat. Cell Biol. 105 (10), 567–574. https://doi.org/10.1038/NCB1719.

Nian, M., Huo, X., Zhang, Jiangtao, Mao, Y., Jin, F., Shi, Y., Jun, Zhang, 2022. Association of emerging and legacy per- and polyfluoroalkyl substances with unexplained recurrent spontaneous abortion. Ecotoxicol. Environ. Saf. 239, 113691 https://doi.org/10.1016/J.ECOENV.2022.113691.

Niu, Z., Iyer, D., Conway, S.J., Martin, J.F., Ivey, K., Srivastava, D., Nordheim, A., Schwartz, R.J., 2008. Serum response factor orchestrates nascent sarcomerogenesis and silences the biomineralization gene program in the heart. Proc. Natl. Acad. Sci. U. S. A. 105, 17824. https://doi.org/10.1073/PNAS.0805491105.

Ou, Y., Zeng, X., Lin, S., Bloom, M.S., Han, F., Xiao, X., Wang, H., Matala, R., Li, X., Qu, Y., Nie, Z., Dong, G., Liu, X., 2021. Gestational exposure to perfluoroalkyl substances and congenital heart defects: a nested case-control pilot study. Environ. Int. 154, 106567 https://doi.org/10.1016/J.ENVINT.2021.106567.

Preston, C.C., Wyles, S.P., Reyes, S., Storm, E.C., Eckloff, B.W., Faustino, R.S., 2018. NUP155 insufficiency recalibrates a pluripotent transcriptome with network remodeling of a cardiogenic signaling module. BMC Syst. Biol. 12, 1–13. https://doi.org/10.1186/S12918-018-0590-X/FIGURES/5.

Pusapati, G.V., Hughes, C.E., Dorn, K.V., Zhang, D., Sugianto, P., Aravind, L., Rohatgi, R., 2014. EFCAB7 and IQCE regulate hedgehog signaling by tethering the EVC-EVC2 complex to the base of primary cilia. Dev. Cell 28, 483. https://doi.org/10.1016/J.DEVCEL.2014.01.021.

Rasmussen, M.A., Holst, B., Tümer, Z., Johnsen, M.G., Zhou, S., Stummann, T.C., Hyttel, P., Clausen, C., 2014. Transient p53 suppression increases reprogramming of human fibroblasts without affecting apoptosis and DNA damage. Stem Cell Reports 3, 404–413. https://doi.org/10.1016/J.STEMCR.2014.07.006.

Ritchie, M.E., Phipson, B., Wu, D., Hu, Y., Law, C.W., Shi, W., Smyth, G.K., 2015. Limma powers differential expression analyses for RNA-sequencing and microarray studies. Nucleic Acids Res. 43, e47 https://doi.org/10.1093/NAR/GKV007.

Rosenmai, A.K., Ahrens, L., le Godec, T., Lundqvist, J., Oskarsson, A., 2018. Relationship between peroxisome proliferator-activated receptor alpha activity and cellular concentration of 14 perfluoroalkyl substances in HepG2 cells. J. Appl. Toxicol. 38 https://doi.org/10.1002/jat.3515.

Rouhani, F., Kumasaka, N., de Brito, M.C., Bradley, A., Vallier, L., Gaffney, D., 2014. Genetic background drives transcriptional variation in human induced pluripotent stem cells. PLoS Genet. 10, e1004432 https://doi.org/10.1371/JOURNAL.PGEN.1004432.

Ruiz-Villalba, A., Hoppler, S., van den Hoff, M.J.B., 2016. Wnt signaling in the heart fields: variations on a common theme. Dev. Dyn. 245, 294–306. https://doi.org/10.1002/DVDY.24372.

Schrenk, D., Bignami, M., Bodin, L., Chipman, J.K., del Mazo, J., Grasl-Kraupp, B., Hogstrand, C., Hoogenboom, L., Leblanc, J.C., Nebbia, C.S., Nielsen, E., Ntzani, E., Petersen, A., Sand, S., Vleminckx, C., Wallace, H., Barregård, L., Ceccatelli, S., Cravedi, J.P., Halldorsson, T.I., Haug, L.S., Johansson, N., Knutsen, H.K., Rose, M., Roudot, A.C., Van Loveren, H., Vollmer, G., Mackay, K., Riolo, F., Schwerdtle, T., 2020. Risk to human health related to the presence of perfluoroalkyl substances in food. EFSA J. 18 https://doi.org/10.2903/j.efsa.2020.6223.

Shi, X., Zhang, Y., Gong, Y., Chen, M., Brand-Arzamendi, K., Liu, X., Wen, X.Y., 2021. Zebrafish hhatla is involved in cardiac hypertrophy. J. Cell. Physiol. 236, 3700–3709. https://doi.org/10.1002/JCP.30106.

Smoak, I.W., Byrd, N.A., Abu-Issa, R., Goddeeris, M.M., Anderson, R., Morris, J., Yamamura, K., Klingensmith, J., Meyers, E.N., 2005. Sonic hedgehog is required for cardiac outflow tract and neural crest cell development. Dev. Biol. 283, 357–372. https://doi.org/10.1016/J.YDBIO.2005.04.029.

Smyth, G.K., 2004. Linear models and empirical bayes methods for assessing differential expression in microarray experiments. Stat. Appl. Genet. Mol. Biol. 3 https://doi.org/10.2202/1544-6115.1027/MACHINEREADABLECITATION/RIS.

Tang, L.L., Wang, J.D., Xu, T.T., Zhao, Z., Zheng, J.J., Ge, R.S., Zhu, D.Y., 2017. Mitochondrial toxicity of perfluorooctane sulfonate in mouse embryonic stem cell-derived cardiomyocytes. Toxicology 382, 108–116. https://doi.org/10.1016/J.TOX.2017.03.011.

Thibodeaux, J.R., Hanson, R.G., Rogers, J.M., Grey, B.E., Barbee, B.D., Richards, J.H., Butenhoff, J.L., Stevenson, L.A., Lau, C., 2003. Exposure to Perfluorooctane sulfonate during pregnancy in rat and mouse. I: maternal and prenatal evaluations. Toxicol. Sci. 74, 369–381. https://doi.org/10.1093/TOXSCI/KFG121.

van Welie, I., du Lac, S., 2011. Bidirectional control of BK channel open probability by CAMKII and PKC in medial vestibular nucleus neurons. J. Neurophysiol. 105, 1651. https://doi.org/10.1152/JN.00058.2011.

Villar, A.V., García, R., Llano, M., Cobo, M., Merino, D., Lantero, A., Tramullas, M., Hurlé, J.M., Hurlé, M.A., Nistal, J.F., 2013. BAMBI (BMP and activin membrane-bound inhibitor) protects the murine heart from pressure-overload biomechanical stress by restraining TGF-β signaling. Biochim. Biophys. Acta - Mol. Basis Dis. 1832, 323–335. https://doi.org/10.1016/J.BBADIS.2012.11.007.

Wiegering, A., Rüther, U., Gerhardt, C., 2017. The role of hedgehog Signalling in the formation of the ventricular septum. J. Dev. Biol. 5 https://doi.org/10.3390/JDB5040017.

Wikström, S., Lin, P.I., Lindh, C.H., Shu, H., Bornehag, C.G., 2020. Maternal serum levels of perfluoroalkyl substances in early pregnancy and offspring birth weight. Pediatr. Res. 87, 1093. https://doi.org/10.1038/S41390-019-0720-1.

Xia, W., Wan, Y., Li, Y., Yuan Zeng, H., Lv, Z., Li, G., Wei, Z., Xu, S. Qing, 2011. PFOS prenatal exposure induce mitochondrial injury and gene expression change in hearts of weaned SD rats. Toxicology 282, 23–29. https://doi.org/10.1016/j.tox.2011.01.011.

Yang, R., Liu, S., Liang, X., Yin, N., Ruan, T., Jiang, L., Faiola, F., 2020. F–53B and PFOS treatments skew human embryonic stem cell in vitro cardiac differentiation towards epicardial cells by partly disrupting the WNT signaling pathway. Environ. Pollut. 261, 114153 https://doi.org/10.1016/j.envpol.2020.114153.

Yu, J., Vodyanik, M.A., Smuga-Otto, K., Antosiewicz-Bourget, J., Frane, J.L., Tian, S., Nie, J., Jonsdottir, G.A., Ruotti, V., Stewart, R., Slukvin, I.I., Thomson, J.A., 2007. Induced pluripotent stem cell lines derived from human somatic cells. Science (80-.) 318, 1917–1920. https://doi.org/10.1126/SCIENCE.1151526/SUPPL_FILE/YU.SOM.REVISION.1.PDF.

Zeng, H., Cai, He, Zhi, Q., Li, Y. Yuan, Wu, C. Qiu, Wu, Y. Mou, Xu, S. Qing, 2015. Prenatal exposure to PFOS caused mitochondia-mediated apoptosis in heart of weaned rat. Environ. Toxicol. 30, 1082–1090. https://doi.org/10.1002/TOX.21981.

Zhang, Y.Y., Tang, L.L., Zheng, B., Ge, R.S., Zhu, D.Y., 2016. Protein profiles of cardiomyocyte differentiation in murine embryonic stem cells exposed to perfluorooctane sulfonate. J. Appl. Toxicol. 36, 726–740. https://doi.org/10.1002/JAT.3207.

Zhu, H., 2016. Forkhead box transcription factors in embryonic heart development and congenital heart disease. Life Sci. 144, 194–201. https://doi.org/10.1016/J.LFS.2015.12.001.